International Journal of Thermophysics, Vol. 20, No. 2, 1999

Equation of State and Thermodynamic Properties of Pure D_2O and $D_2O + H_2O$ Mixtures in and Beyond the Critical Region

S. B. Kiselev,[1-3] I. M. Abdulagatov,[1,4] and A. H. Harvey[1]

Received July 9, 1998

A parametric crossover model is adapted to represent the thermodynamic properties of pure D_2O in the extended critical region. The crossover equation of state for D_2O incorporates scaling laws asymptotically close to the critical point and is transformed into a regular classical expansion far from the critical point. An isomorphic generalization of the law of corresponding states is applied to the prediction of thermodynamic properties and the phase behavior of $D_2O + H_2O$ mixtures over a wide region around the locus of vapor–liquid critical points. A comparison is made with experimental data for pure D_2O and for the $D_2O + H_2O$ mixture. The equation of state yields a good representation of thermodynamic property data in the range of temperatures $0.8T_c(x) \leqslant T \leqslant 1.5T_c(x)$ and densities $0.35\rho_c(x) \leqslant \rho \leqslant 1.65\rho_c(x)$.

KEY WORDS: binary mixtures; critical region; D_2O; equation of state; H_2O; phase behavior; thermodynamic properties.

1. INTRODUCTION

In addition to being of practical interest (primarily in the nuclear industries), the thermodynamic properties of heavy water and its mixtures with ordinary water are interesting from a modeling point of view. Because

[1] Physical and Chemical Properties Division, National Institute of Standards and Technology, 325 Broadway, Boulder, Colorado 80303, U.S.A.

[2] To whom correspondence should be addressed.

[3] Present address: Chemical Engineering and Petroleum Refining Department, Colorado School of Mines, Golden, Colorado 80401-1887, U.S.A.

[4] Permanent address: Institute for Geothermal Problems of the Dagestan Scientific Center of the Russian Academy of Sciences, Kalinina Ave. 39-A, Makhachkala 367030, Dagestan, Russia.

0195-928X/99/0300-0563$16.00/0

of the similarity of the molecules, the mixture properties are very nearly ideal. Reproducing the small nonidealities is a challenge for modelers. In addition, the presence of the isotope exchange equilibrium involving HDO adds an extra complication, but does so in a way that has less impact on the phase diagram than is observed in most reacting systems.

In this work, we focus on the region near the critical locus of the mixture by applying a previously developed parametric crossover model. We begin with an exposition of the renormalized Landau expansion that has been used in some crossover models and show its connections with the parametric model used here. We then apply the parametric model to pure D_2O and compare the results to PVT, phase boundary, and caloric data. Finally, the model is applied to the binary mixture and compared with the limited data that exist in the applicable range of the model.

2. CROSSOVER FREE ENERGY FOR PURE FLUIDS

2.1. Renormalized Landau Expansion

The classical approach to the study of critical phenomena was developed by Landau [1]. The Landau, or mean-field, theory is based on the introduction of an order parameter $\Delta\eta$ which is zero in the more symmetric (disordered) phase and nonzero in the less symmetric (ordered) phase [1, 2]. The free energy of the system in the mean-field theory is written in the form

$$\bar{A}(T, \rho) = \Delta\bar{A}(\tau, \Delta\eta) + (\rho/\rho_c)\,\bar{\mu}_0(T) + \bar{A}_0(T) \tag{1}$$

where $\Delta\eta$ is the order parameter, $\tau = T/T_c - 1$ is the dimensionless difference of the temperature T from the critical temperature T_c, $\Delta\bar{A}$ is the critical part of the dimensionless Helmholtz free energy density $\bar{A} = \rho A/P_c$, while $\bar{\mu}_0(T)$ and $\bar{A}_0(T)$ are analytic functions of temperature. In the critical region, $|\tau| \ll 1$ and $|\Delta\eta| \ll 1$, and the critical part of the free energy, $\Delta\bar{A}$, is represented in the Landau theory by a Taylor expansion in powers of the order parameter [1],

$$\Delta\bar{A}(\tau, \Delta\eta) = \hat{a}_{12}\tau\,\Delta\eta^2 + \hat{a}_{04}\,\Delta\eta^4 \tag{2}$$

where $\hat{a}_{12}$ and $\hat{a}_{04}$ are system-dependent coefficients. For one-component fluids the dimensionless difference of the density ρ from the critical density ρ_c can be chosen as the order parameter, $\Delta\eta = \Delta\rho = \rho/\rho_c - 1$. The dimensionless chemical potential $\Delta\bar{\mu} = (\partial(\Delta\bar{A})/\partial\Delta\rho)_\tau$, conjugate to the order parameter $\Delta\rho$, plays the role of the ordering field. In the Landau theory, the equilibrium value of the order parameter on the coexistence curve,

$\Delta\rho_{exs}$, is proportional to $|\tau|^{1/2}$ and the susceptibility $\bar{\chi}=(\partial\Delta\eta/\partial\Delta\bar{\mu})_\tau$, diverges as τ^{-1} at $\rho=\rho_c$, while the specific heat $\bar{C}_V=-(\partial^2\bar{A}/\partial\tau^2)_{\Delta\eta}$ remains finite at the critical point [1]. Thus, for the Landau (or mean-field) theory, the critical exponents are

$$\beta_L=\tfrac{1}{2}, \qquad \gamma_L=1, \qquad \text{and} \qquad \alpha_L=0 \tag{3}$$

The Landau theory is valid only in the temperature region $Gi \ll |\tau| \ll 1$, where the long-range fluctuations in the order parameter are negligible [1, 2]. Here $Gi \propto (\bar{l}/l_0)^6$ is the Ginzburg number, $\bar{l}$ is an average distance between particles, and l_0 is an effective average radius of the interaction between molecules. The intensity of the fluctuations diverges at the critical point, and at temperatures $|\tau| \ll Gi$, the fluctuations as given by renormalization-group (RG) theory should be considered. According to RG theory, the fluctuations close to the critical point renormalize Eq. (2) into [3–6]

$$\Delta\bar{A}(\tau, \Delta\eta)=\hat{a}_{12}\tau Y^{-\alpha/2\Delta_1}\Delta\eta^2 Y^{(\gamma-2\beta)/2\Delta_1}+\hat{a}_{04}\Delta\eta^4 Y^{(\gamma-2\beta)/\Delta_1}-\mathcal{K}(\tau^2) \tag{4}$$

where Y denotes a crossover function to be specified below, while the kernel term $\mathcal{K}(\tau^2)$, which provides the correct scaling behavior of the isochoric specific heat asymptotically close to the critical point, has the form,

$$\mathcal{K}(\tau^2)=\hat{a}_{20}\tau^2(Y^{-\alpha/\Delta_1}-1) \tag{5}$$

In these equations $\gamma=1.24$, $\beta=0.325$, $\alpha=2-\gamma-2\beta=0.110$, and $\Delta_1=0.51$ are the current best estimates of the nonclassical critical exponents [7, 8]. In the mean-field regime at $Gi \ll |\tau| \ll 1$, the crossover function $Y \to 1$ and Eq. (4) is transformed into the Landau expression [Eq. (2)].

Unfortunately, the solution of the RG equations, except in special cases, cannot be obtained rigorously without additional approximations. Nicoll et al. [4, 6] obtained an exact solution of these equation for the spherical model

$$Y^{-1}=1+\bar{u}\left[\left(\frac{\Lambda}{\kappa}\right)^{\omega}-1\right] \tag{6}$$

where $\kappa^2=[\partial\Delta\bar{A}/\partial(\Delta\eta^2 Y^{(\gamma-2\beta)/2\Delta_1})]_\tau$, and the high-wavenumber cutoff Λ and the coefficient $\bar{u}$ are system-dependent parameters. In the spherical model, the critical exponent $\omega=1$ and the mean-field limit, at which the crossover function $Y=1$, is not achieved asymptotically as $(\Lambda/\kappa)\to 0$ but, rather, is reached abruptly as $(\Lambda/\kappa)\to 1$. Therefore, the spherical-model crossover function (6) cannot be used in the renormalized Landau expansion (4) for thermodynamic calculations in fluids and fluid mixtures.

In order to apply the RG result to real fluids, Chen and co-workers [9, 10] replaced the parameter (Λ/κ) in Eq. (6) by $[1+(\Lambda/\kappa)^2]^{1/2}$. From different approximations for the critical exponents as functions of the renormalized coupling in the RG equations, five approximations for the crossover function Y were obtained [11]. The simplest phenomenologically repaired crossover function, referred to as crossover model I by Tang et al. [11], is

$$Y=\{1+\bar{u}[(1+\Lambda^2/\kappa^2)^{\omega/2}-1]\}^{-1} \tag{7}$$

where $\omega=\Delta_1/\nu=0.8095$ is a universal critical exponent for three-dimensional Ising-like systems. The Ginzburg number in this approach is

$$Gi=\frac{g_0(\bar{u}\Lambda)^2}{c_t(1-\bar{u})^{1/\Delta_1}} \tag{8}$$

where $g_0=0.0314$ is a universal constant and c_t is a system-dependent parameter [12].

Equations (2)–(7) correspond to an Ising-type system, symmetric with respect to the transformation $\Delta\rho\to-\Delta\rho$, $\Delta\mu\to-\Delta\mu$. Fluids exhibit this symmetry only in an extremely small range of temperatures and densities around the critical point [13–16]. The first asymmetric term of order $\tau(\Delta\rho)^3$, which destroys the symmetry of Eq. (2), can be effectively taken into account by a redefinition of the order parameter

$$\Delta\eta=\Delta\rho-d_1\tau \tag{9}$$

where d_1 is the rectilinear diameter amplitude. This is a so-called "trivial" account of the asymmetry [1, 2], which is by itself not sufficient to describe the actual thermodynamic behavior of real fluids because of the long-range fluctuations in the order parameter observed in the critical region. The vapor-liquid asymmetry observed in fluids and fluid mixtures [13, 17] can be taken into account in fluctuation theory by a "mixing" of the chemical potential and the temperature-like variables [2, 18, 19], resulting in a singular diameter $\propto|T-T_c|^{1-\alpha}$. Another way is the addition of a new correction term $\propto|T-T_c|^{\beta+\Delta_5}$ for the order parameter $\Delta\eta$ in the two-phase region, which arises from an additional term $\propto\Delta\eta^5$ in the Landau expansion [Eq. (2)] and, as a consequence, in the Landau–Ginzburg–Wilson effective Hamiltonian of the system [3, 20].

As more terms are taken into account in the renormalized Landau expansion [Eq. (4)], a wider range of temperature and density around the critical point can be described with this crossover model. Incorporation of

the crossover function [Eq. (7)] into a six-term Landau expansion [10, 21] has enabled this model to represent the thermodynamic properties of pure fluids over a range bounded by $\bar{\chi} \geqslant 2.2$, which for the critical isochore approximately corresponds to a temperature range $T_c \leqslant T \leqslant 1.2T_c$. With the empirically improved crossover function introduced by Jin et al. [22, 23], the range of the six-term Landau crossover model can be extended up to temperatures $T \leqslant 1.6T_c$. However, even with the empirically improved crossover function, the six-term Landau crossover model is rather complicated. The current parametric crossover model is generally simpler in the sense that few iterative routines are required in its practical implementation, and it has been developed to cover a wider range of the state variables.

2.2. Parametric Crossover Model

A phenomenological procedure for dealing with the crossover behavior of the Helmholtz free energy density has been proposed by Kiselev et al. [24–27]. In this approach, the crossover expression for the critical part of the Helmholtz free energy can be represented in parametric form [27],

$$\Delta\bar{A}(r, \theta) = kr^{2-\alpha}R^{\alpha}(q)\left[a\Psi_0(\theta) + \sum_{i=1}^{5} c_i r^{\Delta_i} R^{-\bar{\Delta}_i}(q)\, \Psi_i(\theta)\right] \tag{10}$$

$$\tau = r(1 - b^2\theta^2) \tag{11}$$

$$\Delta\rho = kr^{\beta}R^{-\beta+1/2}(q)\,\theta + d_1\tau \tag{12}$$

where b^2 is a universal linear-model parameter, and k, d_1, a, and c_i are system-dependent coefficients. The universal scaled functions

$$\Psi_i(\theta) = \sum_{j=0}^{5} \alpha_{ij}\theta^j \qquad (i = 0,..., 5) \tag{13}$$

are the same as those in the parametric crossover model employed earlier by Kiselev et al. [26, 27]. The crossover function $R(q)$,

$$R(q) = \left(1 + \frac{q^{2\Delta_0}}{q_0 + q^{\Delta_0}}\right)^{1/\Delta_0}, \qquad q = rg \tag{14}$$

(where the parameter $g \propto Gi^{-1}$, while q_0 and Δ_0 are universal constants, initially taken to be unity [24]) is a simple Padé approximant of the crossover free-energy obtained from the numerical solution of the renormalization-group equations [28, 29]. As pointed out in Ref. 30, for the case

$q_0 = 0$ and $\Delta_0 = \Delta_1$, the crossover function $R(q)$ as given by Eq. (14) coincides exactly with the crossover function $Y^{1/\Delta_1}(q)$ obtained recently by Belyakov et al. [31] in the first order ε-expansion. However, the form of the crossover equations obtained in Ref. 31 differs from Eqs. (10)–(12); therefore, we will use in Eq. (14) the values [27]

$$q_0 = 1, \qquad \text{and} \qquad \Delta_0 = \tfrac{1}{2} \tag{15}$$

With this value of the exponent Δ_0, the crossover equation [Eq. (10)] reproduces the square-root corrections to the isochoric specific heat arising in the mean-field regime at $q \gg 1$ ($Gi \ll |\tau| \ll 1$) from an additional gradient term in the Landau expansion for the effective Hamiltonian of the system [1].

The first three terms on the right-hand side of Eq. (10) correspond to the asymptotic ($i = 0$) and first and second correction terms ($i = 1, 2$) in the Wegner expansion for three-dimensional Ising-like systems [17, 32]:

$$\Delta\bar{A}(\tau, \Delta\rho) = k\tau^{2-\alpha}\left[\bar{a} f_0(\Delta\rho/|\tau|^{\beta}) + \sum_{i=1}^{4} \bar{c}_i \tau^{\Delta_i} f_i(\Delta\rho/|\tau|^{\beta})\right] \tag{16}$$

where $f_i(\Delta\rho/|\tau|^{\beta})$ are universal scaled functions, and k, $\bar{a}$, and $\bar{c}_i$ are critical amplitudes. The next two asymmetric terms in Eq. (10) ($i = 3$ and $i = 4$) are equivalent to a "mixing" of the thermodynamic variables [15], and the last term in Eq. (10) ($i = 5$) corresponds to the additional asymmetric term $\propto \Delta\eta^5$ in the effective Hamiltonian of the system [3, 20]

As demonstrated in previous work [26, 30], the crossover function Y in the renormalized Landau expansion [Eq. (4)] can be defined through the crossover function $R(q)$ as

$$Y(q) = [q/R(q)]^{\Delta_1} \tag{17}$$

For large values of the variable q at $|\tau| \gg Gi$, the crossover function $R(q)$ modifies each term in Eq. (10) so they all become analytic, and Eq. (10) is transformed into the renormalized Landau expansion with additional asymmetric terms proportional to $\tau\,\Delta\eta^3$, $\tau^2\,\Delta\eta$, and η^5 as discussed above. Thus, the parametric crossover model given by Eqs. (10)–(12) is physically equivalent to the six-term crossover model [10, 21] and the effectiveness of either crossover model is determined largely by the choice of the crossover function. Our parametric crossover model is specified by Eqs. (10)–(14) and contains the following universal constants: the critical exponents α, β, Δ_i, and $\tilde{\Delta}_i$ and the linear-model parameter b^2. The values of all universal constants are listed in Table I, and the universal scaled functions $\Psi_i(\theta)$ are given in Table II.

Table I. Universal Constants

$\alpha = 0.110$
$\beta = 0.325$
$\gamma = 2 - \alpha - 2\beta = 1.24$
$b^2 = (\gamma - 2\beta)/\gamma(1 - 2\beta) = 1.359$
$\Delta_1 = \tilde{\Delta}_1 = 0.51$
$\Delta_2 = \tilde{\Delta}_2 = 2\Delta_1 = 1.02$
$\Delta_3 = \Delta_4 = \gamma + \beta - 1 = 0.565$
$\Delta_5 = 1.19$
$\tilde{\Delta}_3 = \tilde{\Delta}_4 = \Delta_3 - 1/2 = 0.065$
$\tilde{\Delta}_5 = \Delta_5 - 1/2 = 0.69$
$e = 2\gamma + 3\beta - 1$
$e_1 = (5 - 2e)(e - \beta)(3 - 2e)/3(5\beta - e)$
$e_2 = (5 - 2e)(e - 3\beta)/3(5\beta - e)$
$e_3 = 2 - \alpha - \Delta_5$
$e_4 = (5 - 2e_3)(e_3 - 3\beta)/3(5\beta - e_3)$

3. CROSSOVER FREE ENERGY FOR BINARY MIXTURES

In accordance with the principle of critical-point universality with appropriately chosen thermodynamic variables, also called isomorphic variables, the thermodynamic potential of a binary mixture has the same form as the thermodynamic potential of a one-component fluid [19, 33–35]. In the present paper we use the thermodynamic variables adopted by Kiselev and co-workers [27, 36–38]. The isomorphic free-energy density of a binary mixture is given by

$$\rho\tilde{A}(T, \rho, \tilde{x}) = \rho A(T, \rho, x) - \rho\tilde{\mu}x(T, \rho, \tilde{x}) \tag{18}$$

where $\tilde{\mu} = \mu_2 - \mu_1$ is the difference between the chemical potentials μ_1 and μ_2 of the mixture components, and $x = N_2/(N_1 + N_2)$ is the mole fraction of the second component in the mixture. The isomorphic variable $\tilde{x}$ is

Table II. Universal Scaled Functions

$\Psi_0(\theta) = (1/2b^4)[2\beta(b^2 - 1)/(2 - \alpha) + 2\beta(2\gamma - 1)(1 - b^2\theta^2)/(\gamma(1 - \alpha)) + (2\beta - 1)(1 - b^2\theta^2)^2/\alpha]$
$\Psi_1(\theta) = [1/(2b^2(1 - \alpha + \Delta_1))][(\gamma + \Delta_1)/(2 - \alpha + \Delta_1) - (1 - 2\beta)\, b^2\theta^2]$
$\Psi_2(\theta) = [1/(2b^2(1 - \alpha + \Delta_2))][(\gamma + \Delta_2)/(2 - \alpha + \Delta_2) - (1 - 2\beta)\, b^2\theta^2]$
$\Psi_3(\theta) = \theta - (2/3)(e - \beta)\, b^2\theta^3 + e_1(1 - 2\beta)\, b^4\theta^5/(5 - 2e)$
$\Psi_4(\theta) = (1/3)\, b^2\theta^3 + e_2(1 - 2\beta)\, b^4\theta^5/(5 - 2e)$
$\Psi_5(\theta) = (1/3)\, b^2\theta^3 + e_4(1 - 2\beta)\, b^4\theta^5/(5 - 2e_3)$

related to the field variable ζ, first introduced by Leung and Griffiths [39], by the relation,

$$\tilde{x} = 1 - \zeta = \frac{e^{\tilde{\mu}/RT}}{1 + e^{\tilde{\mu}/RT}} \tag{19}$$

The thermodynamic equation,

$$x = -\tilde{x}(1-\tilde{x})\left(\frac{\partial \tilde{A}}{\partial \tilde{x}}\right)_{T,\rho} \frac{1}{RT} \tag{20}$$

(where R is the molar gas constant) relates the mole fraction x to the isomorphic variable $\tilde{x}$. At fixed $\tilde{x}$, the isomorphic free energy $\rho\tilde{A}$ will be the same function of τ and ρ as the Helmholtz free-energy density of a one-component fluid. Based on the crossover equation of state for a pure fluid [Eqs. (10)–(14)], the isomorphic free-energy density of a binary mixture is

$$\frac{\rho\tilde{A}(T,\rho,\tilde{x})}{R\rho_{c0}T_{c0}} = \tilde{k}r^{2-\alpha}[R(q)]^{\alpha}\left[\tilde{a}\Psi_0(\theta) + \sum_{i=1}^{5}\tilde{c}_i r^{\Delta_i}[R(q)]^{-\Delta_i}\Psi_i(\theta)\right] + \sum_{i=1}^{4}\left(\tilde{A}_i + \frac{\rho}{\rho_c}\tilde{m}_i\right)\tau^i(\tilde{x}) - \frac{P_c(\tilde{x})}{R\rho_{c0}T_{c0}} + \frac{\rho T}{\rho_{c0}T_{c0}}[\ln(1-\tilde{x}) + \tilde{m}_0] \tag{21}$$

$$\tau = \frac{T - T_c(\tilde{x})}{T_c(\tilde{x})} = r(1 - b^2\theta^2) \tag{22}$$

$$\Delta\rho = \frac{\rho - \rho_c(\tilde{x})}{\rho_c(\tilde{x})} = \tilde{k}r^{\beta}[R(q)]^{-\beta+1/2}\theta + \tilde{x}_1\tau \tag{23}$$

In Eqs. (21)–(23), all system-dependent parameters as well as the critical parameters $T_c(\tilde{x})$, $\rho_c(\tilde{x})$, and $P_c(\tilde{x})$ are analytic functions of the isomorphic variable $\tilde{x}$. For these functions, we use the same expressions as Kiselev et al. [27, 38, 40]

$$T_c(\tilde{x}) = T_{c0}(1-\tilde{x}) + T_{c1}\tilde{x} + \tilde{x}(1-\tilde{x})\sum_{i=0}^{3} T_i(1-2\tilde{x})^i \tag{24}$$

$$\rho_c(\tilde{x}) = \rho_{c0}(1-\tilde{x}) + \rho_{c1}\tilde{x} + \tilde{x}(1-\tilde{x})\sum_{i=0}^{3} \rho_i(1-2\tilde{x})^i \tag{25}$$

$$P_c(\tilde{x}) = P_{c0}(1-\tilde{x}) + P_{c1}\tilde{x} + \tilde{x}(1-\tilde{x})\sum_{i=0}^{2} P_i(1-2\tilde{x})^i \tag{26}$$

where subscripts c0 and c1 correspond to the first and second components of the mixture, respectively. In addition to Eqs. (24)–(26), we also adopt a critical-line condition of the form [27, 38, 40],

$$\frac{d\tilde{m}_0}{d\tilde{x}} = \frac{1}{R\rho_c T_c}\frac{dP_c}{d\tilde{x}} + (\tilde{A}_1 + \tilde{m}_1)\frac{\rho_{c0}}{\rho_c}\frac{T_{c0}}{T_c^2}\frac{dT_c}{d\tilde{x}} \tag{27}$$

$$T_c(\tilde{x}) = T_c(x), \qquad \rho_c(\tilde{x}) = \rho_c(x), \qquad P_c(\tilde{x}) = P_c(x) \tag{28}$$

The critical-line condition implies that the zero of the chemical potential of a binary mixture can be chosen so that the isomorphic variable $\tilde{x} = x$ along the entire critical line, including the one-component limits.

To specify the crossover equation for $\tilde{A}(T, \rho, \tilde{x})$ of a binary mixture, we also need the system-dependent parameters $\tilde{d}_1(\tilde{x})$, $\tilde{k}(\tilde{x})$, $\tilde{a}(\tilde{x})$, $\tilde{c}_i(\tilde{x})$, $\tilde{g}(\tilde{x})$, $\tilde{m}_i(\tilde{x})$, and $\tilde{A}_i(\tilde{x})$ as functions of the isomorphic variable $\tilde{x}$. To represent all these system-dependent parameters in Eqs. (21)–(23), represented as $\tilde{k}_i(\tilde{x})$, as functions of $\tilde{x}$, we use an isomorphic generalization of the law of corresponding states [27, 40]. The isomorphic generalization of the law of corresponding states assumes that all system-dependent parameters depend on $\tilde{x}$ only through the excess critical compressibility factor $\Delta Z_c(\tilde{x})$, where

$$\Delta Z_c(\tilde{x}) = Z_c(\tilde{x}) - Z_{cid}(\tilde{x}) \tag{29}$$

is the difference between the actual critical compressibility factor of a mixture $Z_c(\tilde{x}) = P_c(\tilde{x})/R\rho_c(\tilde{x})\, T_c(\tilde{x})$ and its "ideal" part $Z_{cid}(\tilde{x}) = Z_{c0}(1-\tilde{x}) + Z_{c1}\tilde{x}$. The dimensionless coefficients $\tilde{k}$, $\tilde{g}$, and $\tilde{d}_1$ are written in the form

$$\tilde{k}_i(\tilde{x}) = k_{i0} + (k_{i1} - k_{i0})\,\tilde{x} + k_i^{(1)}\,\Delta Z_c(\tilde{x}) \tag{30}$$

and all other coefficients are given by

$$\tilde{k}_i(\tilde{x}) = \frac{P_c(\tilde{x})}{R\rho_{c0}T_{c0}}\left[k_{i0} + (k_{i1} - k_{i0})\,\tilde{x} + k_i^{(1)}\,\Delta Z_c(\tilde{x})\right] \tag{31}$$

In the context of the law of corresponding states, the mixing coefficients $k_i^{(1)}$ in Eqs. (30) and (31) are universal constants for all binary mixtures of simple fluids [27, 40]. For mixtures with $\Delta Z_c > 0.06$, one needs to use an extended version of the law of corresponding states with additional terms quadratic in $\Delta Z_c(\tilde{x})$ [40]. However, since for the $D_2O + H_2O$ mixture $\max\{\Delta Z_c\} \ll 0.06$, we use expressions linear in $\Delta Z_c(\tilde{x})$. In the present paper, for the mixing coefficients $k_i^{(1)}$, we adopt the same values employed earlier for methane + ethane and ethane + *n*-butane mixtures

Table III. Mixture Constants

	D_2O	H_2O	$k_i^{(1)}$
	Critical amplitudes		
k	1.47247	1.41380	−3.4826
d_1	-7.85398×10^{-1}	-7.13319×10^{-1}	-6.7567×10^{-1}
a	2.32676×10	2.25385×10	-2.3130×10
c_1	−2.75293	−6.83712	-3.3449×10
c_2	9.36745	1.33215×10	0
c_3	-1.41504×10	-1.16219×10	−1.1514
c_4	9.23419	7.83568	2.1111×10
	Crossover parameter		
g	1.55062×10^{-2}	1.80152×10^{-5}	9.8900
	Background coefficients		
A_1	−7.94392	−7.81074	9.0968
A_2	1.88718×10	1.81122×10	-3.3379×10
A_3	2.18830	2.72022	0
$\Delta m_1 = m_{11} - m_{10}$	0	0	3.4252
m_1	-2.41636×10	-2.07384×10	-2.6928×10^2
m_2	-1.31765×10	-1.14168×10	1.7328×10
m_3	1.46961×10	6.23749	−5.9960
m_4	-1.32875×10	−6.41886	0

[27]. The values of the coefficients are listed in Table III. The relevant thermodynamic derivatives of the crossover free energy are summarized in the Appendix.

4. CROSSOVER FREE ENERGY FOR PURE D_2O

In order to use the parametric crossover model defined by Eqs. (21)–(23) for pure D_2O ($\tilde{x} = x = 0$), it is necessary to have the critical parameters T_c, ρ_c, and P_c. For D_2O we adopted the values recommended by Levelt Sengers et al. [43], as accepted by the International Association for the Properties of Water and Steam, but with the critical temperature converted to ITS-90:

$$T_c = 643.847 \text{ K}, \qquad \rho_c = 356 \text{ kg} \cdot \text{m}^{-3}, \qquad P_c = 21.671 \text{ MPa} \tag{32}$$

We then fit experimental PVT data in the range of temperatures and densities bounded by

$$\tau + 1.2\Delta\rho^2 \leqslant 0.5, \qquad T \geqslant 0.98 T_c \tag{33}$$

in order to obtain the fluid-specific critical amplitudes (the rescaled asymptotic critical amplitude k, the rectilinear diameter amplitude d_1 of the coexistence curve, the amplitude a of the asymptotic term, the amplitudes c_i $(i=1,...,5)$ of the nonasymptotic terms, and the inverse rescaled Ginzburg number g), and background coefficients A_i. We also used in the fit two vapor pressure data from Ref. 44 at temperatures of approximately $0.9T_c$ and $0.85T_c$. The PVT data were taken from Refs. 45–47. The experimental PVT data of Rivkin and Akhundov [45, 46] refer to a sample with 0.13 mol% H_2O and the experimental data of Tsederberg et al. [47] to a sample with 0.20 mol% H_2O. Therefore, we applied a small impurity correction to the data as described by Kamgar-Parsi et al. [48]. Figure 1 shows the percentage deviations of the experimental pressures from the calculated values as a function of temperature and density. Inside the region specified by Eq. (33), the parametric crossover model represents the experimental PVT data with an average absolute deviation (AAD) of about 0.09%. The pressure deviations correspond approximately to those found by Kamgar-Parsi et al. [48]. The coefficients resulting from the fit are given in Table III. The coefficient g for D_2O in Table III is much smaller then 1. Therefore, heavy water, like pure H_2O, is essentially a nonclassical "scaling" system, and a crossover to mean-field classical behavior in the region given by Eq. (33) is never observed.

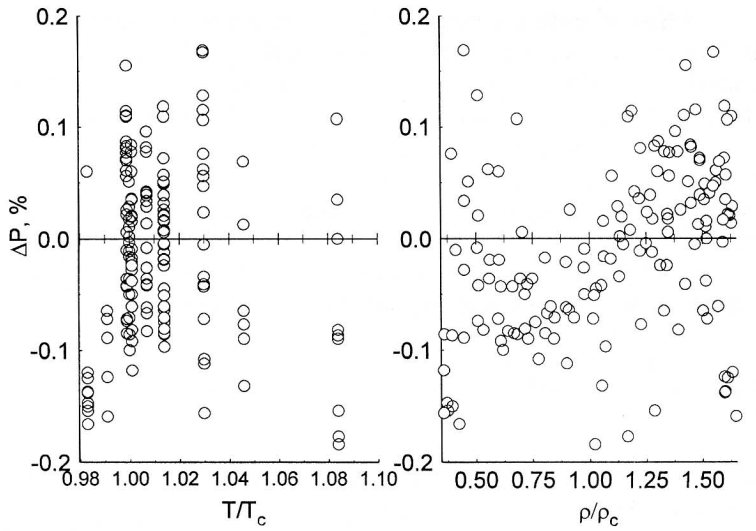

Fig. 1. Percentage deviations of the experimental pressures obtained by Rivkin and Akhundov [45, 46] for D_2O from values calculated with the crossover equation of state.

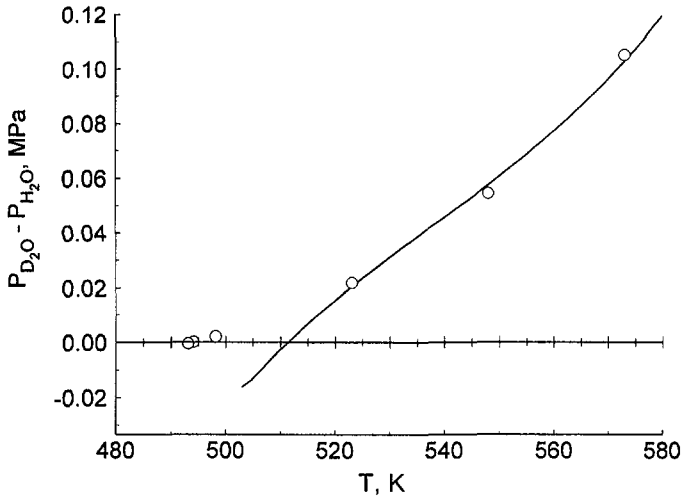

Fig. 2. The vapor pressure difference $P_{D_2O} - P_{H_2O}$ as a function of temperature. The symbols indicate experimental data of Liu and Lindsay [44], and the curves represent values calculated with the crossover model.

Figure 2 shows the calculated difference between the vapor pressure of D_2O and that of ordinary water [53] as a function of temperature, along with data for this quantity from Liu and Lindsay [44]. The agreement for this sensitive quantity is excellent down to perhaps 520 K; at lower temperatures the crossover model exceeds its range of validity (for both pure components), and its accuracy is diminished. In particular, the model gives equality of the vapor pressures (such a crossing of vapor-pressure curves is called a Bancroft point) at 511 K, whereas the experimental value is approximately 494 K.

The coefficients $\tilde{m}_i$ are found from caloric data. $\tilde{m}_0$ and $\tilde{m}_1$ determine the values of the entropy and the enthalpy at the critical point [30]:

$$\frac{S_c}{R} = -\frac{\rho_{c0} T_{c0}}{\rho_c T_c}(\tilde{A}_1 + \tilde{m}_1) - \tilde{m}_0, \quad \text{and} \quad \frac{H_c}{RT_{c0}} = -\frac{\rho_{c0}}{\rho_c}(\tilde{A}_1 + \tilde{m}_1) \tag{34}$$

which can be chosen arbitrarily. In this work we set $\tilde{m}_0 = 0$ and found the coefficient $\tilde{m}_1$ from Eqs. (34), where for the critical enthalpy H_c we adopted the same value as Kamgar-Parsi et al. [48],

$$H_c = 1.9546 \times 10^3 \text{ kJ} \cdot \text{kg}^{-1} \tag{35}$$

The coefficients $\tilde{m}_i$ for $i \geqslant 2$ determine the background contributions to the isochoric specific heat and can be determined from fitting either heat capacity or sound speed data. Unfortunately, there are no sound-speed data in the critical region for D_2O. Therefore, we found the coefficients $\tilde{m}_2$, $\tilde{m}_3$, and $\tilde{m}_4$ from a fit of the crossover model to the isochoric specific heat data obtained by Amirkhanov et al. [49] at two near-critical isochores, and experimental data of Mursalov [50] at other isochores. The resulting values for $\tilde{m}_i$ are given in Table III.

Experimental isochoric heat capacity data reported by Mursalov [50] for heavy water cover a temperature range from 294 to 747 K and densities between 52.466 and 1104.972 $kg \cdot m^{-3}$. Measurements were made for 23 isochores in the one- and two-phase regions including eight near-critical isochores: $\rho = 219.298$, 261.097, 303.030, 338.409, 344.828, 370.370, 400.000, and 492.611 $kg \cdot m^{-3}$. Measurements were made using a high-temperature and high-pressure constant-volume adiabatic calorimeter. The temperature was measured by a platinum resistance thermometer (PTS-10) which was calibrated within an accuracy of ± 1 mK at VNIFTRI (Moscow) on the IPTS-68 temperature scale; therefore, we converted Mursalov's C_v data to the ITS-90 temperature scale.

The calorimeter was a multilayer system and consisted of an inner thin-walled vessel with 0.5 mm thick and 60 mm in diameter and an outer

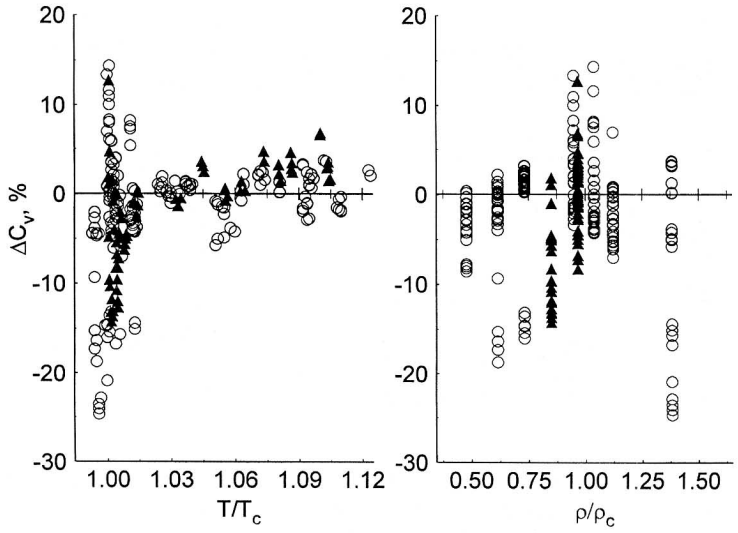

Fig. 3. Percentage deviations of the experimental isochoric specific heats obtained by Amirkhanov et al. [49] (triangles) and by Mursalov [50] (circles) for D_2O from values calculated with the crossover equation of state.

spherical shell 7 mm thick. The inner volume of the calorimeter is $100.58 \pm 0.05\ cm^3$. The results of C_v measurements by this method depend on the values of the temperature-dependent empty-calorimeter heat capacity C_0. C_0 was determined experimentally using water and nitrobenzene as standard fluids at temperatures up to 423.15 K. At high temperatures ($T > 423.15$ K), the values of C_0 were measured using C_P data of air at atmospheric pressure. The heat capacities at atmospheric pressure for these fluids are known with an accuracy of ± 0.2 to 0.3%. Therefore, the values of the empty calorimeter heat capacity C_0 were determined with an uncertainty of $\pm 0.3\%$ at temperatures up to 423.15 K, and 2 to 2.5% at high temperatures ($T \geqslant 470$ K). The average value of C_0 for this calorimeter is about $44.0\ J \cdot K^{-1}$, which was not more than 15 to 20% of the total heat capacity of the system calorimeter + heavy water. With this value of C_0, Mursalov [50] estimated the experimental uncertainty of the isochoric

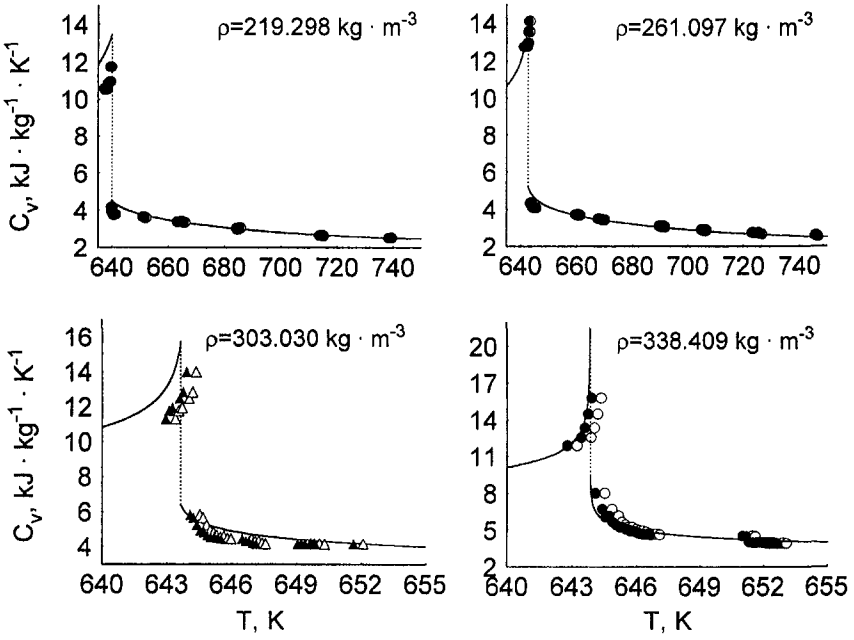

Fig. 4. The isochoric specific heat data obtained by Amirkhanov et al. [49] (triangles) and by Mursalov [50] (circles) for D_2O at isochores $\rho = 219.298$, 261.097, 303.030, and 338.409 $kg \cdot m^{-3}$ as a function of temperature compared with predictions of the crossover equation of state (curves). The empty symbols correspond to the experimental temperatures [49, 50] on ITS-90, and the filled symbols indicate values with the temperature scale lowered by 0.45 K.

specific heat to be 2% far from the critical point, and 3.5 to 4.5% in the critical region.

Figure 3 shows the percentage deviations of the experimental isochoric specific heats from the calculated values as a function of temperature and density in the one-phase region. Except for the near-critical isotherms at $0.98T_c \leqslant T \leqslant 1.02T_c$, where deviations approach 20%, the parametric crossover model represents the experimental C_v data with an AAD of about 2% inside the region specified by Eq. (33), corresponding approximately to the experimental uncertainty in this region. In Figs. 4 and 5 we show a comparison of calculated and experimental isochoric specific heats along the individual isochores. For isochores $\rho = 219.298$, 261.097, 303.030, 338.409, 370.370, 400.000, and 492.611 $kg \cdot m^{-3}$ in the temperature range from the saturation value T_s to $T_s + 2$ K or $T_s < T < 645$ K, the experimental C_v data are represented by the crossover equation of state to within $\pm 15\%$. At isochores $\rho = 370.370$ and 338.409 $kg \cdot m^{-3}$, near the phase transition,

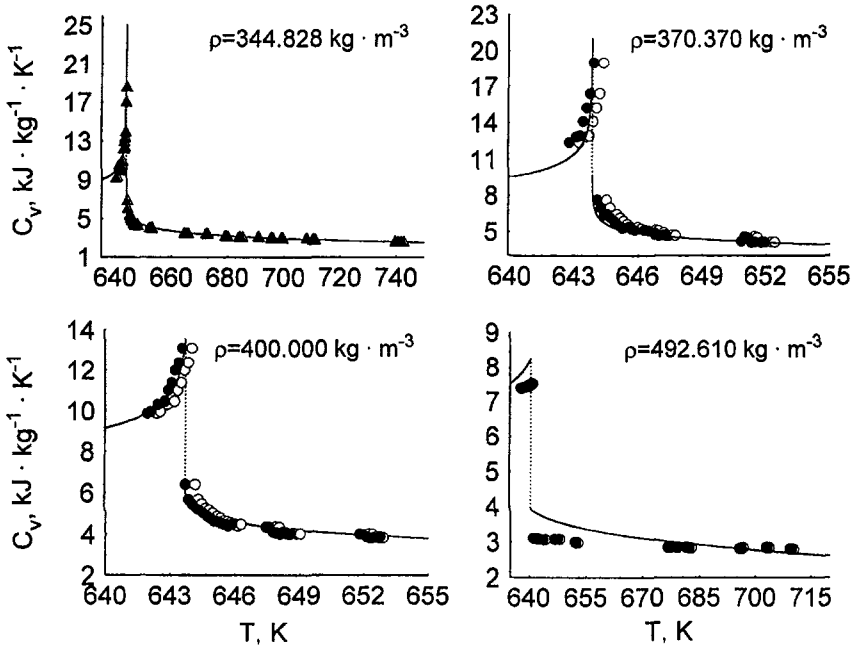

Fig. 5. The isochoric specific heat data obtained by Amirkhanov et al. [49] (triangles) and by Mursalov [50] (circles) for D_2O at isochores $\rho = 344.828$, 370.370, 400.000, and 492.610 $kg \cdot m^{-3}$ as a function of temperature compared with predictions of the crossover equation of state (curves). The open symbols correspond to the experimental temperatures [49, 50] on ITS-90, and the filled symbols indicate values with the temperature scale lowered by 0.45 K.

all data exhibit systematically higher deviations, while for the isochores $\rho = 219.298$, 261.097, and 492.611 kg · m^{-3}, systematically lower deviations are observed. For all isochores, the saturation temperatures $T_s(\rho)$ show systematic deviations of about $\Delta T = 0.455$ K. The value of the critical temperature obtained by Mursalov [50] is also 0.45 K higher than T_c as given in Eq. (32). These temperature deviations could be a consequence of incorrect calibration of the platinum resistance thermometer (PTS-10). The thermometer resistances at 0 and 100°C reported by Mursalov [50] were $R_0 = 10.123\ \Omega$ and $R_{100}/R_0 = 1.3924$, while the standard value is $R_{100}/R_0 = 1.3920$. Therefore, all experimental temperatures in the one- and two-phase regions were shifted by 0.45 K. With the shifted temperatures, agreement within ±2% between experimental and calculated values of C_v is observed for isochores $\rho = 170.387$, 303.030, and 400.000 kg · m^{-3} in the entire temperature range from $T_s(\rho)$ up to 739.623 K. Only 5 points of 90 show deviations of about +10%. Large systematic negative deviations of about 10 to 15% are also observed for most isochores in the two-phase region near the phase transition temperatures. Only for two isochores, $\rho = 219.298$ and 303.030 kg · m^{-3}, in the immediate vicinity of the phase transition temperatures, do the deviations increase to 20 to 25%.

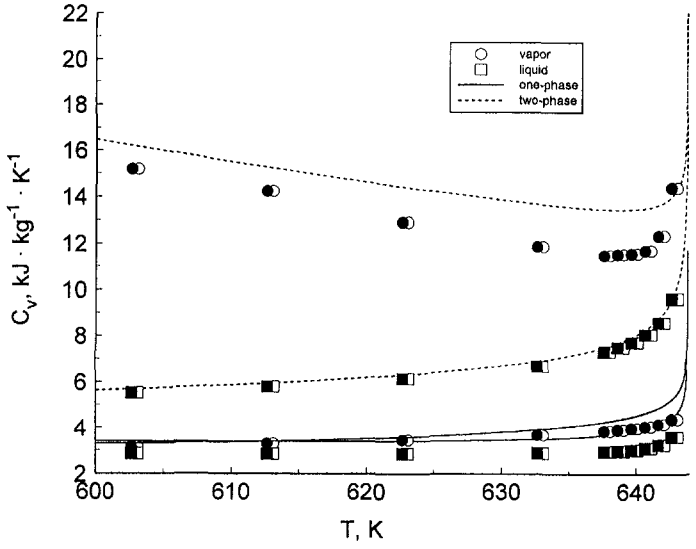

Fig. 6. The isochoric specific heat data obtained by Mursalov [50] for D_2O at the coexistence curve as a function of temperature compared with predictions of the crossover equation of state (curves). The open symbols correspond to the experimental temperatures [50] on ITS-90, and the filled symbols indicate values with the temperature scale lowered by 0.45 K.

Figure 6 gives a comparison of the experimental data with the calculated values of the isochoric specific heats as functions of temperature along the coexistence curve in the one- and two-phase regions. All experimental C_v data in the two-phase region are systematically lower than calculated values. Since the derivatives dC_v/dT_s and $d\rho/dT_s$ are large in the critical region, even small deviations in T_s result in large deviations in C_v and saturated densities in the critical region. The corrections in C_v and saturated density due to the temperature shift $\Delta T = T_s(\text{shift}) - T_s(\text{exp})$ can be estimated from the simplified equations,

$$\Delta C_v = \Delta T \frac{dC_v}{dT} \quad \text{and} \quad \Delta\rho = \Delta T \frac{d\rho}{dT} \tag{36}$$

For example, at $T = 643$ K and $\Delta T = 0.45$ K, the value of ΔC_v is about 8.65% for the isochore $\rho = 344.828\ \text{kg} \cdot \text{m}^{-3}$, and about 16.4% at $\rho = 370.370\ \text{kg} \cdot \text{m}^{-3}$. At temperatures between 640 and 643 K, the values of $\Delta\rho$ vary between 2 and 9%, while at temperatures $T \geqslant 643.5$ K, values of $\Delta\rho$ increase up to 12.35% and more. The corrections due to the temperature shift are negligible at densities and temperatures far from the

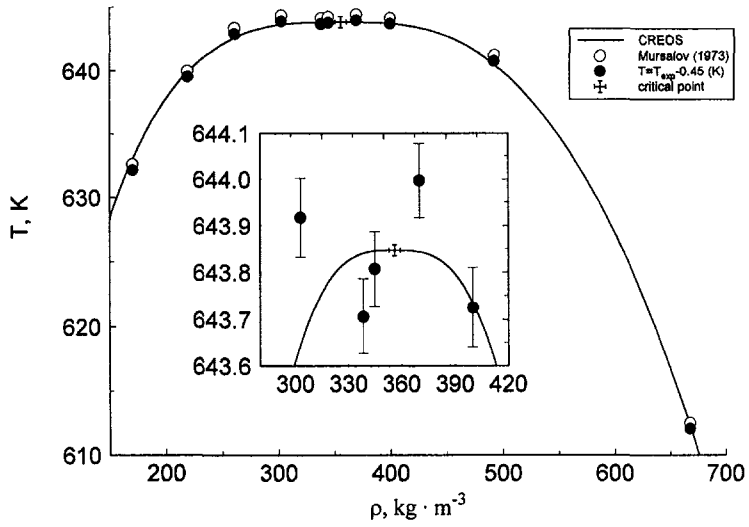

Fig. 7. The saturation temperatures T_s obtained by Mursalov [50] for D_2O at the coexistence curve as a function of density compared with predictions of the crossover equation of state (curve). The open symbols correspond to the experimental temperatures [50] on ITS-90, and the filled symbols indicate values with the temperature scale lowered by 0.45 K.

critical point. For example, for isochores $\rho = 344.828$ and 370.370 $kg \cdot m^{-3}$ at 640 K, this correction in C_v is about 0.8 to 1.23%. As shown in Fig. 6, the original C_v data in the two-phase region deviate by about 15 to 20%, while the corrected values agree with the crossover EOS within 5 to 6%. The original saturation temperatures extracted from the experimental C_v data of Mursalov [50] and those shifted by 0.45 K as a function of density are shown in Fig. 7. One can see that, with the temperature shift, the experimental data are in good agreement with the calculated values of the saturated density.

A comparison of the predictions of the crossover model with the experimental C_P data of Rivkin and Egorov [51, 52] is shown in Figs. 8 and 9. At pressures $P = 22.065$, 23.536, and 24.516 MPa, a small systematic deviation from the experimental data, connected with a difference of the actual locations of the experimental and calculated C_P maxima, is observed in Fig. 9 (see inset). Kamgar-Parsi et al. [48] found the same small mismatch between the densities calculated for the experimental data points and those corresponding to the predicted C_P values. They found that this mismatch disappears if the temperatures associated with the experimental C_P data of Rivkin and Egorov [51, 52] are shifted by 0.11 K. Since we, unlike Kamgar-Parsi et al. [48], did not use the experimental C_P data in

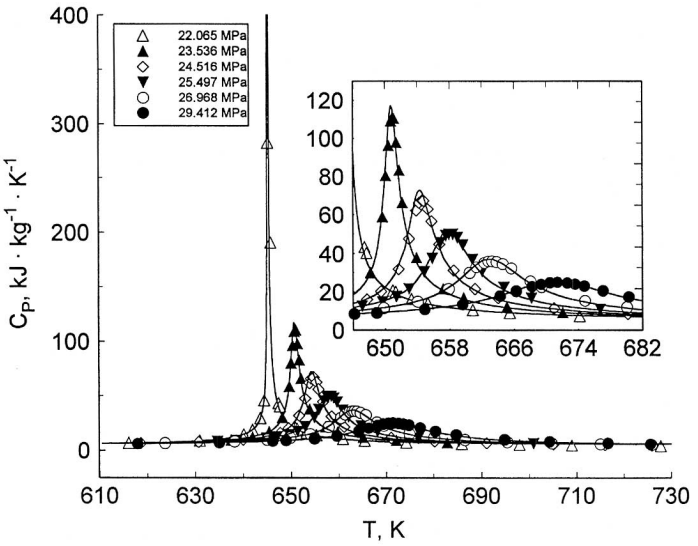

Fig. 8. The isobaric specific heat data of Rivkin and Egorov [51, 52] (symbols) for D_2O along isobars as a function of temperature compared with predictions of the crossover equation of state (curves).

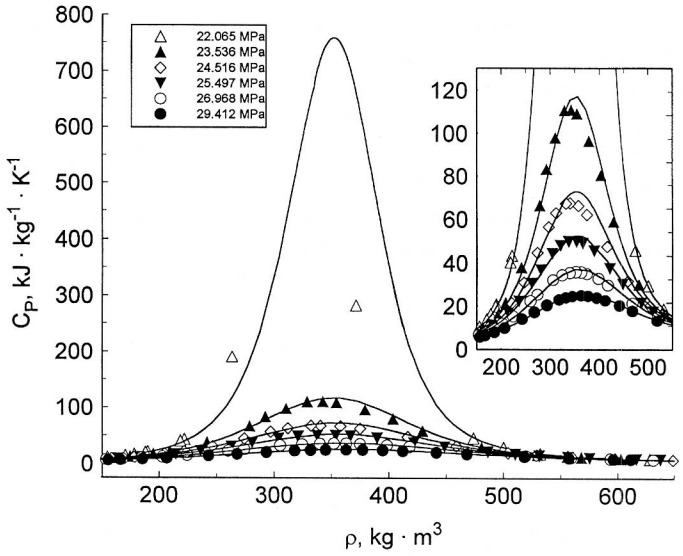

Fig. 9. The isobaric specific heat data obtained by Rivkin and Egorov [51, 52] (symbols) for D_2O at isobars as a function of density compared with predictions of the crossover equation of state (curves).

the fitting procedure, we represent the experimental data of Rivkin and Egorov [51, 52] with the original temperatures, but converted to ITS-90.

5. CROSSOVER FREE ENERGY MODEL FOR THE D_2O+H_2O MIXTURE

Once the pure-fluid equations of state for the components of a binary mixture are known, only the critical locus of the binary mixture is needed in order to predict the phase behavior of the mixture. It is not necessary to fit additional experimental data [27, 40]. For pure D_2O, we used parameters found in the previous section, while for pure H_2O we adopted the parameters obtained recently by Kiselev and Friend [53]. These parameters are listed in Table III.

Unfortunately, we do not know the critical locus for the D_2O+H_2O mixture. Only a few data points [54] on the T_c-x curve are available, and this is not sufficient information to determine all of the adjustable parameters required in Eqs. (24)–(26). Experimental T_c-x data obtained by Marshall and Simonson [54] indicate that the critical temperature of the D_2O+H_2O mixture may be described with a linear interpolation

between the two pure-fluid critical temperatures. Since there was no information about the critical pressure and the critical density for the mixture, we adopted the same linear interpolations for the $P_c - x$ and $\rho_c - x$ curves. Thus, we set all mixing coefficients T_i, ρ_i, and P_i in Eqs. (24)–(26) to zero.

The law of corresponding states crossover model was successfully applied recently by Kiselev and co-workers to VLE surfaces and one-phase supercritical PTp data [40–42] and to excess enthalpies and enthalpy increments of a number of binary mixtures [30]. The $D_2O + H_2O$ mixture differs from the mixtures considered previously by the presence of the isotope-exchange equilibrium,

$$D_2O + H_2O \rightleftharpoons 2DHO \tag{37}$$

Kiselev et al. [55] recently proposed a constructive approach for the incorporation of chemical reaction in the crossover model for the Helmholtz free energy. In this approach, a chemical reaction can be incorporated in Eqs. (21)–(23) by considering the coefficients $\tilde{k}_i$ as functions of the extent of the reaction. As a consequence, with chemical equilibrium all coefficients in Eqs. (21)–(23) become more complicated functions of the field variable $\tilde{x}$ than in the nonreacting systems. Therefore, in the present paper we renormalized the mixing coefficients Δm_1 and $k_{m_1}^{(1)}$ in Eq. (31) for the

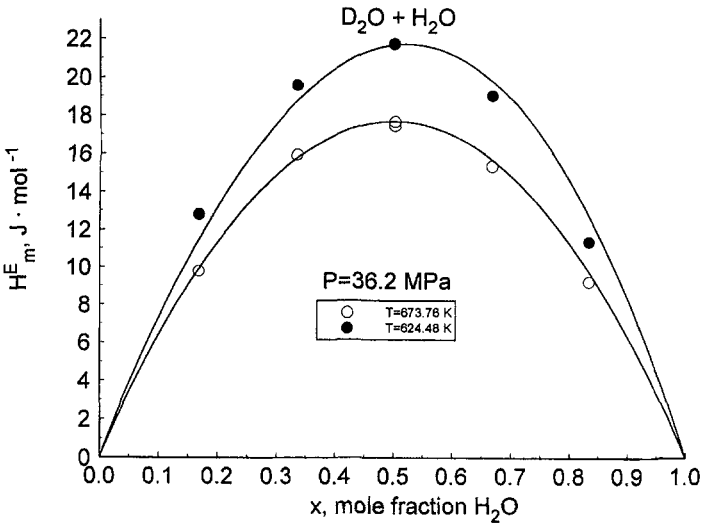

Fig. 10. Excess enthalpy H_m^E for $D_2O + H_2O$ mixtures at temperatures of 673.76 and 624.48 K at 36.2 MPa as a function of composition. Curve corresponds to the crossover model, and symbols indicate the experimental data of Simonson [56].

parameter $\tilde{m}_1$, which determines the critical locus of the enthalpy $H_c(x)$ in binary mixtures [see Eq. (34)]. For this purpose, the experimental excess enthalpies of D_2O+H_2O mixtures measured by Simonson [56] were used. The renormalized values of the coefficients Δm_1 and $k_{m_1}^{(1)}$ are presented in Table III.

Figure 10 compares the excess enthalpies calculated from the crossover model with values obtained by Simonson [56] at two temperatures at a pressure of 36.2 MPa. Agreement is good, even though at the lower of the two temperatures, the experimental densities are about twice the critical density; the crossover model is not expected to work as well so far from the critical density.

It would be of interest to evaluate the performance of the model for vapor–liquid equilibrium (VLE) calculations in the mixture. Unfortunately, we know of no experimental VLE data at temperatures high enough for our crossover model to be quantitatively valid. The only data at moderately high temperatures are those of Zieborak [57], whose measurements extend to the region where the mixture exhibits an azeotrope (due to the crossing of the vapor–pressure curves at the Bancroft point) near 494 K.

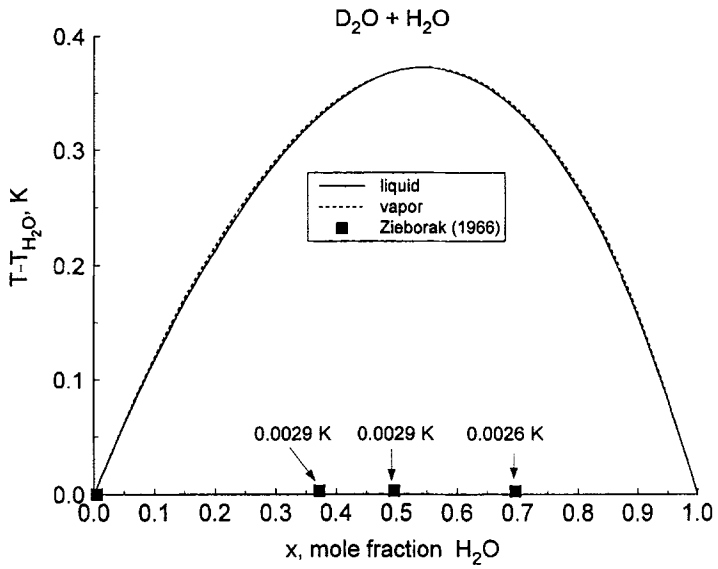

Fig. 11. Vapor–liquid equilibrium temperatures relative to that of pure H_2O for D_2O+H_2O mixtures as a function of composition. The symbols indicate bubble-point data obtained by Zieborak [57], and the curves represent values calculated with the crossover model.

In Fig. 11, we plot the difference in boiling temperature between the mixture and pure H_2O. In order to compare with Zieborak's data, we have plotted them at the pressure where he found the H_2O and D_2O vapor pressures to be equal, and the results of the crossover model are plotted at the (slightly different) pressure where the model predicts the Bancroft point. The model results are qualitatively correct, in that they indicate a nearly symmetric, maximum-boiling azeotrope. However, the results disagree quantitatively, as the model predicts far more nonideality than the very weak azeotrope indicated by the data. Another indication of the quantitative disagreement is that the model predicts azeotropy for an interval of about 40 K above where the vapor pressure curves cross, whereas the data of Zieborak [57] indicate the azeotrope disappears within about 1 K of this point.

6. CONCLUSIONS

We have developed a parametric crossover model, valid in the extended critical region, for heavy water and its mixtures with ordinary water. The results for caloric, PVT, and phase-equilibrium properties of pure D_2O are in good agreement with experimental data.

For mixtures of heavy water with ordinary water, there are few data in the region of validity of the model. The model is able to reproduce excess enthalpy data at high temperatures. For phase equilibria, while it is qualitatively correct in predicting a weak maximum-boiling azeotrope, the predicted magnitude of the azeotrope is much too large.

This quantitative disagreement may be because the azeotrope is far enough away from the critical locus to be outside the range of validity of the model. Better results at these conditions might be obtained by applying a theory that crosses over to an equation of state valid far from the critical point, such as the theory recently developed by Kiselev and Friend [58]. Another reason for the disagreement could be that the isotope exchange reaction was only implicitly considered by a variation in mixing parameters rather than being included explicitly. The enthalpy of this reaction is probably the dominant effect in the excess enthalpy of the mixture [56]. Because of the isotope-exchange reaction, this system is actually a ternary mixture (with approximately 50% HDO for a 50–50 mixture), and qualitative features of the equation of state are affected by the extent of the reaction. An approach for incorporating a chemical reaction in the crossover equation of state has been developed recently by Kiselev and coworkers [55]. If the reaction were incorporated more rigorously, the excess enthalpy would be obtained more naturally, and the VLE predictions might also be improved. However, in order to develop a more complete

and accurate theoretical model for this mixture, more experimental data at high temperatures are needed.

APPENDIX: RELEVANT THERMODYNAMIC QUANTITIES

Pressure P and its derivatives,

$$\frac{P(\rho, T, \tilde{x})}{R\rho_{c0}T_{c0}} = \frac{\rho}{\rho_c}\left(\frac{\partial \Delta\tilde{A}}{\partial \Delta\rho}\right)_{\tau, \tilde{x}} - \Delta\tilde{A} - \tilde{A}_0 \tag{A1}$$

$$\left(\frac{\partial P}{\partial T}\right)_{\rho, x} = \left(\frac{\partial P}{\partial T}\right)_{\rho, \tilde{x}} + \left(\frac{\partial P}{\partial \tilde{x}}\right)_{\rho, T}\left(\frac{\partial \tilde{x}}{\partial T}\right)_{\rho, x} \tag{A2}$$

$$\left(\frac{\partial P}{\partial \rho}\right)_{T, x} = \left(\frac{\partial P}{\partial \rho}\right)_{T, \tilde{x}} + \left(\frac{\partial P}{\partial \tilde{x}}\right)_{T, \rho}\left(\frac{\partial \tilde{x}}{\partial \rho}\right)_{T, x} \tag{A3}$$

$$\left(\frac{\partial P}{\partial x}\right)_{T, \rho} = \left(\frac{\partial P}{\partial \tilde{x}}\right)_{T, \rho}\left(\frac{\partial \tilde{x}}{\partial x}\right)_{T, \rho} \tag{A4}$$

where the critical part,

$$\Delta\tilde{A}(\tau, \Delta\rho, \tilde{x}) = \tilde{k}r^{2-\alpha}R^{\alpha}(q)\left[\tilde{a}\Psi_0(\theta) + \sum_{i=1}^{4}\tilde{c}_i r^{\Delta_i}R^{-\Delta_i}(q)\,\Psi_i(\theta)\right] \tag{A5}$$

and background contribution,

$$\tilde{A}_0(T, \tilde{x}) = \sum_{i=1}^{4}\tilde{A}_i\tau^i(\tilde{x}) - \frac{P_c(\tilde{x})}{R\rho_{c0}T_{c0}} \tag{A6}$$

Isochoric specific heat capacity $C_{v, x}$,

$$\frac{\rho C_{v, x}(T, \rho, \tilde{x})}{TR\rho_{c0}T_{c0}} = -\left(\frac{\partial^2 \Delta\tilde{A}}{\partial T^2}\right)_{\rho, \tilde{x}} - \left(\frac{\partial^2 \tilde{A}_0}{\partial T^2}\right)_{\tilde{x}} - \frac{\rho}{\rho_{c0}}\left(\frac{\partial^2 \tilde{M}_0}{\partial T^2}\right)_{\tilde{x}} - \left[\left(\frac{\partial^2 \Delta\tilde{A}}{\partial T\,\partial \tilde{x}}\right) + \left(\frac{\partial^2 \tilde{A}_0}{\partial T\,\partial \tilde{x}}\right) + \frac{\rho}{\rho_{c0}}\left(\frac{\partial^2 \tilde{M}_0}{\partial T\,\partial \tilde{x}}\right)\right]\left(\frac{\partial \tilde{x}}{\partial T}\right)_{\rho, x} \tag{A7}$$

with

$$\tilde{M}_0(T, \tilde{x}) = \sum_{i=1}^{4}\tilde{m}_i\tau^i(\tilde{x}) + \frac{\rho_c T}{\rho_{c0}T_{c0}}\left[\ln(1-\tilde{x}) + \tilde{m}_0\right] \tag{A8}$$

Isobaric specific heat capacity $C_{P,x}$,

$$C_{P,x}(T,\rho,\tilde{x}) = C_{v,x}(T,\rho,\tilde{x}) + T\left(\frac{\partial P}{\partial T}\right)^2_{\rho,x}\left(\frac{\partial P}{\partial \rho}\right)^{-1}_{T,x}\rho^{-2} \tag{A9}$$

Sound velocity w_s,

$$w_s(T,\rho,\tilde{x}) = \left[\left(\frac{\partial P}{\partial \rho}\right)_{T,x}\frac{C_{P,x}}{C_{v,x}}\right]^{1/2} \tag{A10}$$

The derivatives,

$$\left(\frac{\partial \tilde{x}}{\partial T}\right)_{\rho,x} = -\left(\frac{\partial x}{\partial T}\right)_{\rho,\tilde{x}}\left(\frac{\partial \tilde{x}}{\partial x}\right)_{\rho,T} \tag{A11}$$

$$\left(\frac{\partial \tilde{x}}{\partial \rho}\right)_{T,x} = -\left(\frac{\partial x}{\partial \rho}\right)_{T,\tilde{x}}\left(\frac{\partial \tilde{x}}{\partial x}\right)_{\rho,T} \tag{A12}$$

where the derivatives $(\partial x/\partial T)_{\rho,\tilde{x}}$, $(\partial x/\partial \rho)_{T,\tilde{x}}$, and $(\partial \tilde{x}/\partial x)_{\rho,T}$ can be obtained analytically from the equation,

$$x = \tilde{x} - \tilde{x}(1-\tilde{x})\frac{\rho_{c0}T_{c0}}{\rho T}\left[\left(\frac{\partial \tilde{A}}{\partial \tilde{x}}\right)_{\rho,T} + \left(\frac{\partial \tilde{A}_0}{\partial \tilde{x}}\right)_T + \frac{\rho}{\rho_{c0}}\left(\frac{\partial \Delta\tilde{M}_0}{\partial \tilde{x}}\right)_T\right] \tag{A13}$$

[here $\Delta\tilde{M}_0 = \tilde{M}_0 - (T/T_{c0})\ln(1-\tilde{x})$], which provides a relationship between concentration x and the isomorphic variable $\tilde{x}$ at fixed temperature T and density ρ.

ACKNOWLEDGMENTS

The authors thank D. G. Friend and J. C. Rainwater for valuable discussions and interest in this work. We are indebted to B. A. Mursalov for providing us with his unpublished experimental data. Two of us (S.B.K. and I.M.A.) also would like to thank the Physical and Chemical Properties Division, National Institute of Standards and Technology, for the opportunity to work as Guest Researchers at NIST during the course of this research.

REFERENCES

1. L. D. Landau and E. M. Lifshitz, *Statistical Physics*, 3rd ed. (Pergamon, New York, 1980).
2. A. Z. Patashinskii and V. L. Pokrovskii, *Fluctuation Theory of Phase Transitions* (Pergamon, New York, 1979).

3. J. F. Nicoll, *Phys. Rev. A* **24**:2203 (1981).
4. J. F. Nicoll and J. K. Bhattacharjee, *Phys. Rev. B* **23**:389 (1981).
5. J. F. Nicoll and P. C. Albright, *Phys. Rev. B* **31**:4576 (1985).
6. J. F. Nicoll and P. C. Albright, *Phys Rev. B* **34**:1991 (1986).
7. J. V. Sengers and J. M. H. Levelt Sengers, *Ann. Rev. Phys. Chem.* **37**:189 (1986).
8. M. A. Anisinzov and S. B. Kiselev, *Sov. Tech. Rev. B Therm. Phys.* **6**:1 (1992).
9. Z. Y. Chen, P. C. Albright, and J. V. Sengers, *Phys. Rev. A* **41**:3161 (1990).
10. Z. Y. Chen, A. Abbaci, S. Tang, and J. V. Sengers, *Phys. Rev. A* **42**:4470 (1990).
11. S. Tang, J. V. Sengers, and Z. Y. Chen, *Physica A* **179**:344 (1991).
12. M. A. Anisimov, S. B. Kiselev, J. V. Sengers, and S. Tang, *Physica A* **188**:487 (1992).
13. F. W. Balfour, J. V. Sengers, M. R. Moldover, and J. M. H. Levelt Sengers, *Phys. Lett. A* **65**:223 (1978).
14. J. V. Sengers and J. M. H. Levelt Sengers, *Int. J. Thermophys.* **5**:195 (1984).
15. S. B. Kiselev, *High. Temp.* **24**:375 (1985).
16. Kh. S. Abdulkadirova, S. B. Kiselev, I. G. Kostyukova, and L. V. Fedyunina, *J. Eng. Phys.* **61**:902 (1991).
17. M. Ley-Koo and M. S. Green, *Phys. Rev. A* **16**:2483 (1977).
18. V. A. Pokrovskii, *Pis'ma Zh. Eksp. Teor. Fiz.* (*Sov. Phys. JETP Lett.*) **17**:219 (1973).
19. R. B. Griffiths and J. C. Wheeler, *Phys. Rev. A* **2**:1047 (1970).
20. J. F. Nicoll and R. K. P. Zia, *Phys. Rev. B* **23**:6157 (1981).
21. J. Luettmer-Strathmann, S. Tang, and J. V. Sengers, *J. Chem. Phys.* **97**:2705 (1992).
22. G. X. Jin, S. Tang, and J. V. Sengers, *Phys. Rev. E* **47**:388 (1993).
23. A. A. Povodyrev, G. X. Jin, S. B. Kiselev, and J. V. Sengers, *Int. J. Thermophys.* **17**:909 (1996).
24. S. B. Kiselev, *High. Temp.* **28**:42 (1990).
25. S. B. Kiselev, I. G. Kostyukova, and A. A. Povodyrev, *Int. J. Thermophys.* **12**:877 (1991).
26. S. B. Kiselev and J. V. Sengers, *Int. J. Thermophys.* **14**:1 (1993).
27. S. B. Kiselev, *Fluid Phase Equil.* **128**:1 (1997).
28. C. Bagnuls and C. Bervillier, *Phys. Rev. B* **32**:7209 (1985).
29. C. Bagnuls and C. Bervillier, *Phys. Rev. B* **35**:3585 (1987).
30. S. B. Kiselev and J. C. Rainwater, *J. Chem. Phys.* **109**:643 (1998).
31. M. Y. Belyakov, S. B. Kiselev, and J. C. Rainwater, *J. Chem. Phys.* **107**:3085 (1997).
32. F. G. Wegner, *Phys. Rev. B* **5**:4529 (1972).
33. W. F. Saam, *Phys. Rev. A* **2**:1461 (1970).
34. M. A. Anisimov, A. V. Voronel, and E. E. Gorodetskii, *Sov. Phys. JETP* **33**:605 (1971).
35. M. E. Fisher, in *Critical Phenomena, Vol. 186, Lecture Notes in Physics*, F. J. W. Hahne, ed. (Springer-Verlag, Berlin, 1982), p. 1.
36. S. B. Kiselev, *High. Temp.* **26**:337 (1988).
37. S. B. Kiselev and A. A. Povodyrev, *Fluid Phase Equil.* **79**:33 (1992).
38. S. B. Kiselev and V. D. Kulikov, *Int. J. Thermophys.* **18**:1143 (1997).
39. S. S. Leung and R. B. Griffiths, *Phys. Rev. A* **8**:2670 (1973).
40. S. B. Kiselev and J. C. Rainwater, *Fluid Phase Equil.* **141**:129 (1997).
41. S. B. Kiselev and M. L. Huber, *Int. J. Refrig.* **21**:64 (1998).
42. S. B. Kiselev, J. C. Rainwater, and M. L. Huber, *Fluid Phase Equil.* **150–151**:469 (1998).
43. J. M. H. Levelt Sengers, J. Straub, K. Watanabe, and P. G. Hill, *J. Phys. Chem. Ref. Data* **14**:193 (1985).
44. C.-T. Liu and W. T. Lindsay, *J. Chem. Eng. Data* **15**:510 (1970).
45. S. L. Rivkin and T. S. Akhundov, *Teploenergetika* **9**:62 (1962).
46. S. L. Rivkin and T. S. Akhundov, *Atomnaya Energiya* **14**:581 (1963).

47. N. V. Tsederberg, A. A. Aleksandrov, T. S. Khasanshin, and D. K. Larkin, *Teploenergetika* **20**:17 (1973).
48. B. Kamgar-Parsi, J. M. H. Levelt Sengers, and J. V. Sengers, *J. Phys. Chem. Ref. Data* **12**:513 (1983).
49. Kh. I. Amirkhanov, G. B. Stepanov, B. A. Mursalov, and O. A. Bui, *Teploenergetika* **22**:68 (1973).
50. B. A. Mursalov, Ph.D. thesis (AZNEFTEChIM, Baku, Azerbaijan, 1973).
51. S. L. Rivkin and B. N. Egorov, *Teploenergetika* **9**:60 (1962).
52. S. L. Rivkin and B. N. Egorov, *Teploenergetika* **10**:75 (1963).
53. S. B. Kiselev and D. G. Friend, *Fluid Phase Equil.* **155**:33 (1999).
54. W. L. Marshall and J. M. Simonson, *J. Chem. Thermodyn.* **23**:613 (1991).
55. S. B. Kiselev, M. Y. Belyakov, and J. C. Rainwater, *Fluid Phase Equil.* **150–151**:439 (1998).
56. J. M. Simonson, *J. Chem. Thermodyn.* **22**:739 (1990).
57. K. Zieborak, *Z. Phys. Chem.* **231**:248 (1966).
58. S. B. Kiselev and D. G. Friend, *Fluid Phase Equil.* (in press).